Acta Chemica Scandinavica A 38 (1984) 359–376

Synthesis and Structural, Magnetic, and ESR Characterization of the Tri- and Tetranuclear Hydroxo-Bridged Chromium(III) Ammine Complexes $[Cr_3(NH_3)_{10}(OH)_4]Br_5 \cdot 3H_2O$, $[Cr\{(OH)_2Cr(NH_3)_4\}_3]Br_6 \cdot aq$ and $[Cr_4(NH_3)_{12}(OH)_6]Cl_6 \cdot 4H_2O$ (Rhodoso Chloride)

PETER ANDERSEN,* TURE DAMHUS, ERIK PEDERSEN * and ASBJØRN PETERSEN

Chemistry Department I (Inorganic Chemistry), University of Copenhagen, H.C. Ørsted Institute, Universitetsparken 5, DK-2100 Copenhagen Ø, Denmark

The tri- and tetranuclear hydroxo-bridged chromium(III) ammine complexes $[Cr_3(NH_3)_{10}(OH)_4]Br_5 \cdot 3H_2O$, $[Cr\{(OH)_2Cr(NH_3)_4\}_3]Br_6 \cdot aq$ and $[Cr_4(NH_3)_{12}(OH)_6]Cl_6 \cdot 4H_2O$ have been synthesized reproducibly by treating aqueous $Cr(II)-NH_4^+/NH_3$ buffer solutions with charcoal. The first two compounds were isolated by ion-exchange chromatography. Identifications were performed using X-ray techniques and cleavage of the hydroxo bridges in 70 % $HClO_4$ followed by ESR identification of the resulting mononuclear fragments. The crystal structure of $[Cr_3(NH_3)_{10}(OH)_4]Br_5 \cdot 3H_2O$ was determined from three-dimensional X-ray data collected at room temperature. It crystallizes in the space group $P\bar{1}$ with two formula units in the cell of dimensions $a=8.913(3)$ Å, $b=10.216(4)$ Å, $c=17.423(6)$ Å, $\alpha=104.63(2)°$, $\beta=91.47(2)°$, and $\gamma=114.03(2)°$. The structure was refined to a final value of the conventional R factor (on F) of 0.048 based on 2090 independent observations. The cation consists of a triangular system of chromium atoms bridged by one di-μ-hydroxo and two mono-μ-hydroxo groups. The tetramers were shown by powder X-ray techniques to be analogous to Werner's brown salt and identical to Jørgensen's rhodoso, respectively. The magnetic susceptibilities and ESR spectra were interpreted in terms of sums of two-center interactions including biquadratic terms according to the Heisenberg-Dirac-VanVleck Hamiltonian, using a new program for any number of arbitrary spins based on Wigner-Racah algebra. All interactions were found to be antiferromagnetic. The coupling constants were correlated with structural information. The ground states found in the trinuclear complex and in the analogue of the brown salt were a spin quartet and a septet, respectively. In rhodoso chloride either a triplet or a singlet was found, depending on the coupling model assumed.

In earlier works[1,2] we studied the equilibria in aqueous solution between chromium(III) and nitrogen ligands such as ammonia and ethylenediamine (en). Such solutions are prepared using the combined catalytic effect of chromium(II) and charcoal. Under appropriate conditions a high content of polynuclear species is obtained, and we isolated and characterized several salts of new hydroxo-bridged polynuclear ethylenediamine chromium(III) complexes.[3]

As a natural extension of this work we here present an investigation of some of the condensation products of chromium(III) ammines in aqueous solution. Such solutions were obtained by treating $Cr(II)-NH_4^+/NH_3$ buffer solutions with charcoal, this synthetic method being a small modification of the catalytic procedure mentioned above.

* To whom correspondence should be addressed.

0302-4377/84 $2.50

Obviously this investigation has many points of resemblance with the ethylenediamine work[3] and supplementary details are found there. Thus, our main tool of isolation of pure salts has been ion-exchange chromatography, and as to identification the primary methods have been X-ray diffraction and cleavage of the hydroxo bridges with 70 % $HClO_4$. In this medium the bridges can be cleaved quantitatively without the breaking of any Cr–N bonds, and ESR spectra of the resulting mixture of aqua ions provided an analysis of the mononuclear constituents derived from the bridged complexes.

The tri- and tetranuclear complexes described here were obvious targets for magnetic investigation. The aims were, firstly, to see if the magnetic exchange interactions could be described in terms of sums of two-center interactions, secondly, to see whether the magnitude of such interactions could be correlated with structural information according to the model proposed by Glerup, Hodgson, and Pedersen for superexchange in di-μ-hydroxo-chromium(III) dimers.[4]

EXPERIMENTAL

Preparations. *$[Cr_4(NH_3)_{12}(OH)_6]Br_6 \cdot 2H_2O$ (I)* (rhodoso). Under oxygen-free circumstances 26 g of >99.99 % pure chromium metal were dissolved in 160 ml 9 M HBr and 60 ml water giving a blue solution of Cr(II). Under stirring the solution was slowly added to an ice-cooled mixture of 320 ml 12 M NH_3, 300 g NH_4Br, and 2 g charcoal (nitrogen atmosphere), and this mixture was stirred at room temperature until the hydrogen evolution ceased (15–20 h without the admission of air). Then the rhodoso bromide contaminated with charcoal was filtered off and washed with 0.5 M NH_4Br. On the filter the rhodoso bromide was extracted with 200 ml portions of 30 °C water and immediately reprecipitated with solid NH_4Br under cooling. The purified rhodoso bromide was finally filtered off and washed with 1 M HBr (0 °C) and ethanol giving a yield of 33 g (27 %) of the dihydrate. This procedure may be repeated for further purification.

Rhodoso chloride was prepared in a smaller yield in a similar manner using 26 g Cr and 200 ml 8 M HCl; 700 ml 12 M NH_3, 200 g NH_4Cl, and 2–5 g charcoal. After the reaction had finished (overnight) the charcoal was filtered off, and the filtrate was kept at *ca.* 5 °C. After a few weeks crystals of rhodoso chloride tetrahydrate had formed. They were washed free of NH_4Cl with cold 4 M HCl and then washed with ethanol and air-dried.

Cleavage of I with 12 M HCl and isolation of cis-$[Cr(NH_3)_4(H_2O)Cl]Cl_2$ and $[Cr(NH_3)_2(H_2O)_2Cl_2]Cl$. 5 g of I were treated with 5 ml 12 M HCl at room temperature for 20 min. The mixture was cooled to 0 °C and 50 ml ice-cold acetone were added. After 30 min at 0 °C a precipitate containing the cleavage products was filtered off and washed with acetone and ether. The products were separated by extracting this precipitate with 10–20 ml portions of a 1:1 mixture of methanol and ethanol, to 100 ml of which two drops of 12 M HCl had been added. In this way the diammine was removed and when the extracts became colourless, 2.2 g of the red *cis*-$[Cr(NH_3)_4(H_2O)Cl]Cl_2$ (46 % of total Cr) were left on the filter. It could be purified by dissolution in 10 ml 0.1 M HCl followed by filtration and saturation of the filtrate with gaseous HCl at 0 °C. After a day at 5 °C, 1.8 g of purified salt were isolated after filtration and washing with acetone.

The blue-green extracts were evaporated on a watch glass with a fan. After washing with acetone, 2.0 g (45 %) of purple/blue-green dichroitic, blue-green crystals of $[Cr(NH_3)_2(H_2O)_2Cl_2]Cl$ were obtained. The product was purified by dissolution in a 1:4 mixture of 0.1 M HCl and acetone followed by filtration; the filtrate was saturated with gaseous HCl at 0 °C and allowed to stand overnight at 5 °C. Then 1.5 g of purified salt were isolated after filtration and washing with acetone.

$[Cr_3(NH_3)_{10}(OH)_4]Br_5 \cdot 3H_2O$ (II). An amminechromium(II) solution with charcoal was prepared under circumstances similar to those described for the preparation of I. The amounts used were 10.4 g of >99.99 % Cr in 100 ml 6 M HCl; 375 ml 12 M NH_3, 113 g NH_4Cl, and 3 g charcoal in 400 ml water. The reaction $Cr(II)+H(I) \xrightarrow{C} Cr(III)+H(0)$ was allowed to run under stirring and ice-cooling for *ca.* 5 h. Then, when the hydrogen evolution had died out, the reaction flask was placed in the dark at 5–10 °C for 3 d without the admission of air, after which the charcoal was filtered off. The filtrate (*ca.* 900 ml) could be kept for months at 5–10 °C without significant change of the yields of the following preparations.

450 ml of the filtrate were used in the following ion-exchange chromatographic separation where all solutions and water were cooled to *ca.* 5 °C unless otherwise stated. Portions of the 450 ml filtrate were diluted ×25 with water and passed down a column (50 cm×10 cm ∅) with 50 g of Sephadex SP-C 25 under a pressure of *ca.* 0.5 atm

(as in the following, unless otherwise stated like *e.g.* "slowly"). Now 3 l of water and then 4 l of 0.01 M HCl were passed through the column. The chromium-containing resin was now transferred to the top of another column (50 cm×7 cm ∅) with 90 g of Sephadex SP-C 25 and eluted with 0.7 M NaCl/0.001 M HCl until the first orange band had left the column (*ca.* 1 l eluate). At this stage, there was still *ca.* 80 % of the chromium left on the column, while 20 % consisting of mainly mononuclear species had been removed. Further elution with 0.7 M NaCl/0.001 M HCl revealed a well-defined red band followed by a red-violet band with a less well-defined upper limit. These two bands contain the 5+-charged ion of II and $[Cr\{(OH)_2Cr(NH_3)_4\}_3]^{6+}$ (III), respectively. (Sometimes a small violet band preceded these two bands. It will not be dealt with in this publication). During the chromatographic procedure portions of the red eluate were removed, diluted ×7 with water and concentrated on another column (50 cm×7 cm ∅) with 5–10 g Sephadex SP-C 25. This concentrate was washed free of chloride with water, transferred to the last column, 20 cm×2.5 cm ∅, covered with a 0.5–1 cm layer of pure Sephadex, and carefully and slowly eluted with ice-cold 2 M NaI. The more concentrated part of the eluate (*ca.* 60 ml) was cooled in ice and saturated with NaI (*ca.* 75 g). The volume was doubled by the addition of ethanol, and the mixture was kept at 5–10 °C for 1–2 d. The precipitate, consisting of dark red needles, was filtered off, washed free of iodide with ethanol, and air-dried. Yield: 2 g of $[Cr_3(NH_3)_{10}(OH)_4]I_5 \cdot 4H_2O$ (5 % of the total amount of chromium against 14 % in the red band as a whole).

The iodide was transformed into the bromide (II) in one of two ways: (*a*) 200 mg of the iodide were dissolved in *ca.* 5 ml 50 % ethanol under ice-cooling. The solution was filtered and 2.5 g LiBr were slowly added under continuous ice-cooling. Soon after the bromide was isolated, washed once with 50 % ethanol saturated with LiBr, then several times with 96 % ethanol until the washings were free of bromide. After air-drying the yield was 0.10 g (64 % from the iodide). (*b*) a very pure product was obtained by dissolving 200 mg of the iodide in 10 ml water (room temperature) and concentrating it in a 2 cm layer of Sephadex SP-C 25 in a 15 cm×1 cm ∅ column. This concentrate was washed free of iodide with *ca.* 30 ml water and covered with a 3 mm layer of pure resin. It was then slowly eluted with *ca.* 10 ml 2 M LiBr, the more concentrated part of the eluate (*ca.* 1 ml) being collected and cooled in ice for 1 h. The precipitate was filtered off, washed once with 0.5 ml 2 M LiBr and then with small portions of 96 % ethanol until the washings were free of bromide. Yield after air-drying: 0.06 g (38 %) dark, red-violet crystals of II. Bigger crystals for X-ray diffraction were obtained by placing a semi-saturated solution of LiBr in 50 % ethanol in a narrow test tube (0 °C) and on top of this layer another layer of 50 % ethanol saturated with the bromide (II).

$[Cr\{(OH)_2Cr(NH_3)_4\}_3]Br_6 \cdot aq$ (III). The part of the resin containing the red-violet band (in the 7 cm ∅ column mentioned above) was transferred to a 60 cm×3 cm ∅ column and eluted with 2 M NaCl/0.001 M HCl. During this procedure portions of the eluate were removed, diluted ×10–20 with water and concentrated on a column (50 cm×7 cm ∅) with *ca.* 5 g Sephadex SP-C 25. This concentrate was washed free of chloride with water, transferred to a 20 cm×2.5 cm ∅ column and eluted slowly with 2 M NaI (room temperature). The more concentrated part (*ca.* 50 ml) of the eluate was collected, cooled in ice and saturated slowly with NaI (*ca.* 60 g). The volume was doubled by the addition of ethanol, and the mixture was kept for 1–2 d at 5–10 °C. The precipitate was then filtered off, washed free of iodide with ethanol, and air-dried. Yield: 1.0 g of $[Cr\{(OH)_2Cr(NH_3)_4\}_3]I_6 \cdot 4\ H_2O$ (3 % of the total amount of chromium against 11 % in the red-violet band as a whole).

The bromide, III, was prepared from 200 mg of the iodide in ways similar to the preparation of II and in similar yields. It consists of thin, blue-violet, hexagonal looking plates, which in smaller yields could be grown somewhat bigger under more dilute conditions. The number of waters of crystallization is not well-defined, varying between 4 and 8.

Chemical analysis. All the prepared compounds were analyzed, most of them on a microscale (2–5 mg): chromium by atomic absorption spectrophotometry, nitrogen by Kjeldahl, halides (total and ionic) by potentiometry, and water of crystallization thermogravimetrically (compound I). The analyses were all, within 1–2 % relative, in accordance with the formulae given.

Chemicals and apparatus. All chemicals used were reagent grade or of a similar or better quality; the charcoal was a Norit W product. Visible spectra were measured on a Cary 118 spectrophotometer and ESR spectra on a Jeol JES-ME-1X instrument. A Perkin-Elmer 403 apparatus was used for atomic absorption spectrophotometry, and a Picker FACS-1 diffractometer for collecting the single crystal X-ray data.

The magnetic susceptibilities were measured by the Faraday method in the temperature range 1.8–300 K at a field strength of 12 000 Ø.

Preliminary descriptions of the instruments are found elsewhere.[5] Minor adjustments of our temperature scale were made by application of a new internal temperature standard consisting of a 1 % solution of hexaamminechromium(III) ions in the cubic lattice of the diamagnetic hexaamminecobalt(III) iodide. The line widths of ESR spectra of such samples (<2 mT) in the temperature range 3–300 K showed that this solid solution must have a reciprocal static susceptibility varying linearly with the temperature even well below 1 K if no phase transitions occur. At the magnetic field used here the susceptibility was calculated by application of the Brillouin function, and thus no zero-field splitting was assumed.

Hydrolysis with 70 % $HClO_4$. Ca. 5 mg of the compounds II and III (small crystals), respectively, were treated with 5–10 drops of 70 % $HClO_4$ at 70–80 °C for 1–2 h (the rhodoso perchlorate is not soluble enough in this medium for reaction to take place). The mixture was then cooled and diluted with water until the precipitate had dissolved. The volume was doubled by the addition of glycerol, and the ESR spectrum of the frozen glass at −130 to −140 °C was recorded from 0–0.5 T at 9.2 GHz. Such spectra were compared with similar spectra of glasses containing known amounts of the perchlorates of $[Cr(H_2O)_6]^{3+}$, *fac*-$[Cr(NH_3)_3(H_2O)_3]^{3+}$ (Ref. 6), and *cis*-$[Cr(NH_3)_4(H_2O)_2]^{3+}$ (Ref. 7) (these compounds did not change their spectrum after the above described treatment with 70 % $HClO_4$), and in this way it was possible to determine the content of the different mononuclear aquaammines in the reaction mixtures as described elsewhere.[3] The results are given in Figs. 1 and 2.

X-Ray Diffraction. A structure determination of II was carried out by single crystal X-ray diffraction as described in the next section.

Table 1. Crystal data for $[Cr_3(NH_3)_{10}(OH)_4]Br_5 \cdot 3\ H_2O$

Molecular weight of $Cr_3H_{40}N_{10}O_7Br_5$: 847.9

Triclinic: V=1387.$_1$ Å^3
a=8.913(3) Å, b=10.216(4) Å, c=17.423(6) Å
α=104.63(2)°, β=91.47(2)°, γ=114.03(2)°

Density: d_{obs}=2.0$_4$ g/cm^3, d_{calc}=2.029 g/cm^3 for Z=2

μ(Mo$K\alpha$)=83.1 cm^{-1}, F(000)=826

Space group: $P\bar{1}$ (No. 2)

Developed faces: {100}, {010}, {001}, and {1$\bar{1}$0}

Weissenberg and precession photographs with Cu$K\alpha$ radiation were taken for preliminary purposes, space group determination *etc.* Powder photographs were taken using a Guinier camera with Cu$K\alpha$ radiation and with silicon as internal standard; some results are given in Table 4.

Structure determination of II by single crystal X-ray diffraction. (a) Crystal data. Some of the crystal data are given in Table 1. The unit cell dimensions were determined on the diffractometer, using Mo$K\alpha$ radiation (graphite monochromator), from 28 reflections by a least-squares refinement, and they are in agreement with those determined from powder photographs. The density of the crystals was determined by flotation in mixtures of 1-bromonaphthalene and 1,2-dibromoethane.

(b) Data collections. The diffraction data were collected at 22 °C from a single crystal, 0.4×0.2×0.06 mm^3 in the *a*-, *b*-, and *c*-direction, respectively, using graphite monochromated Mo$K\alpha$ radiation. A θ–2θ scan mode was used with a rate of 1°min^{-1} in 2θ. The scan range was asymmetrical from $2\theta_o$–(1.0°+0.346° tan θ) to $2\theta_o$+(1.2°+0.346° tan θ) where $2\theta_o$ is the calculated peak position. Background counts were made for 20 s at each end of the scan range. All the independent reflections with $2.4° < 2\theta < 40°$ were measured. The intensities of four standard reflections measured after every 40 reflections decreased with exposure time. The four different reflections showed almost the same relative decrease (*ca.* 15 %) during the measurements.

The intensity data were corrected for this deterioration, for Lorenz and polarization effects, and a Gaussian numerical integration procedure[8] was used for absorption correction. This resulted in 2586 independent reflections. The 2090 reflections fulfilling the criterion $I > 2\sigma(I)$ were classified as observed and used for the crystallographic calculations ($\sigma(I)$ is the standard deviation calculated by counting statistics).

The following programs were used for computation: the Vanderbilt System[9] for diffractometer operations, an absorption correction program and a data reduction program both of local origin, ORTEP II[10] for illustrations, and the X-RAY System[11] and MULTAN System[12] for crystal structure analysis.

The atomic scattering factors used were those reported by Cromer and Mann[13] for the uncharged atoms. The anomalous dispersion corrections for chromium and bromine were taken from Cromer and Liberman.[14]

(c) Structure determination and refinement. The structure was initially solved from data not corrected for absorption and crystal deterioration. Combination of the three-dimensional Pat-

terson function and direct methods (MULTAN) gave the positions of the five bromine atoms and the three chromium atoms. Subsequent Fourier syntheses gave the positions of the ten nitrogen and eight oxygen atoms (four from OH-bridges and four from water of crystallization). The structure was refined by the method of least squares (2 blocks) minimizing $R'=\Sigma w(|F_o|-K|F_c|)^2$. When the absorption- and decay-corrected data were used in the refinement it became apparent that two of the water oxygen atoms, O7 and O8, were not fully populated. From the peak heights in the difference Fourier their population parameters were estimated to be *ca.* 0.5 (Cr, N, and Br analyses indicate 3–4 waters of crystallization). After a unit weighted refinement where O7 and O8 were refined with isotropic temperature factors and restricted population parameters of 0.5 and the remaining non-hydrogen atoms were refined with anisotropic thermal parameters the *R*-value had decreased to 0.048 (the average shift/error was 0.08 and the maximum shift/error was 0.9 for O7 and O8). The structure refinement was stopped at this stage, as it was judged that no further reliable information could be obtained considering the decay of the crystal. A rough estimate of the positions of the hydrogen atoms of the four OH bridges was obtained from two independent observations, namely from the atoms within normal hydrogen bond distances to O1–O4 and from the highest maxima in the final difference

Table 2. $[Cr_3(NH_3)_{10}(OH)_4]Br_5 \cdot 3\ H_2O$. Final fractional coordinates and thermal parameters with e.s.d. The expressions for the temperature factors are $\exp(-8\pi^2 U \sin^2\theta/\lambda^2)$ for O7 and O8 and $\exp\{-2\pi^2(U_{11}h^2a^{*2}+....+2U_{23}klb^*c^*)\}$ for the other atoms. $U_{eq}=(U_{11}a^{*2}a^2+....+2U_{23}b^*c^*bc\cos a)/3$. The labeling is explained in Fig. 3.

Atom		*x*	*y*	*z*	U_{eq}/U (Å^2×100)
Br1		0.66107(19)	0.30018(18)	0.22696(11)	5.76(13)
Br2		0.9520(2)	0.97699(18)	0.18646(12)	6.33(13)
Br3		0.3272(3)	0.30026(19)	0.40298(10)	6.81(13)
Br4		0.1524(2)	0.8055(2)	0.43909(10)	6.42(13)
Br5		0.7617(3)	0.5149(2)	0.03740(11)	8.09(15)
Cr1		0.2228(2)	0.4788(2)	0.22101(13)	2.86(15)
Cr2		0.3557(3)	0.7914(2)	0.20749(12)	2.73(15)
Cr3		0.6185(2)	0.7313(2)	0.34373(12)	2.69(15)
O1		0.1767(10)	0.6563(9)	0.2527(5)	3.2(5)
O2		0.3733(10)	0.6010(8)	0.1584(5)	2.9(5)
O3		0.4035(10)	0.5558(9)	0.3102(5)	3.4(5)
O4		0.5312(10)	0.8447(9)	0.2964(5)	3.1(5)
O5		0.6892(16)	0.1484(12)	0.3725(7)	8.4(9)
O6		0.380(2)	0.2591(18)	0.0092(9)	13.2(13)
O7	P.P.=0.5	0.304(5)	0.965(4)	0.015(2)	14.8(13)
O8	P.P.=0.5	0.933(6)	0.076(5)	0.012(3)	19.4(17)
N1		0.0233(13)	0.3773(12)	0.1267(7)	4.2(7)
N2		0.0602(14)	0.3706(14)	0.2936(7)	5.1(8)
N3		0.2791(13)	0.2961(12)	0.1761(7)	4.5(8)
N4		0.1806(14)	0.7516(12)	0.1123(6)	4.1(7)
N5		0.3182(14)	0.9789(12)	0.2697(7)	4.5(8)
N6		0.5376(14)	0.9126(12)	0.1477(7)	4.1(7)
N7		0.7113(13)	0.6084(12)	0.3953(7)	3.7(7)
N8		0.8515(13)	0.9198(12)	0.3789(7)	4.5(8)
N9		0.5429(12)	0.8050(12)	0.4507(6)	3.3(7)
N10		0.6979(13)	0.6598(11)	0.2373(6)	3.3(7)
H1	not refined	0.153	0.717	0.298	
H2	not refined	0.337	0.550	0.103	
H3	not refined	0.417	0.498	0.346	
H4	not refined	0.580	0.962	0.320	

Table 3. $[Cr_3(NH_3)_{10}(OH)_4]Br_5 \cdot 3\ H_2O$. Selected bond lengths (Å), contact distances (Å), and bond angles (°) with e.s.d.

Cr1–O1	1.968(11)	Cr3–N9	2.065(11)	
Cr1–O2	1.987(9)	Cr3–N10	2.069(11)	
Cr1–O3	1.963(9)			
Cr2–O1	1.972(9)			
Cr2–O2	1.989(9)			
Cr2–O4	1.975(9)	O1–Cr1–O2	80.8(4)	
Cr3–O3	1.960(7)	O1–Cr2–O2	80.7(4)	
Cr3–O4	1.952(11)	O1–Cr1–O3	93.9(4)	
		O2–Cr1–O3	91.2(3)	
Cr1–N1	2.103(11)	O1–Cr2–O4	94.9(4)	
Cr1–N2	2.101(13)	O2–Cr2–O4	90.4(4)	
Cr1–N3	2.096(13)	O3–Cr3–O4	90.4(4)	
Cr2–N4	2.089(12)			
Cr2–N5	2.109(13)	Cr1–O1–Cr2	99.0(4)	
Cr2–N6	2.085(12)	Cr1–O2–Cr2	97.8(4)	
Cr3–N7	2.109(15)	Cr1–O3–Cr3	134.4(5)	
Cr3–N8	2.116(9)	Cr2–O4–Cr3	134.6(4)	
O1–Br4	3.275(8)	O1–H1	1.0	
O2–Br5	3.328(8)	O2–H2	1.0	
O3–Br3	3.260(10)	O3–H3	1.0	
O4–O5	2.764(13)	O4–H4	1.0	
Angle between	O1–H1	and plane	O1–Cr1–Cr2	27
Angle between	O2–H2	and plane	O2–Cr1–Cr2	50
Angle between	O3–H3	and plane	O3–Cr1–Cr3	16
Angle between	O4–H4	and plane	O4–Cr2–Cr3	2

Fourier map in the vicinity (*ca.* 1 Å) of O1–O4. The positions of these maxima, called H1–H4, are given in Table 2 and the hydrogen bond data are given in Table 3. The OH directions are approximately towards the contact atoms. Due to the reason mentioned above no attempts were made to refine these hydrogen positions.

The final results of the structure analysis are given in Tables 1–3 and Fig. 3. Lists of thermal parameters and of observed and calculated structure amplitudes are available from the authors upon request.

PARAMETRIZATION OF SUSCEPTIBILITY DATA

The susceptibility data were fitted to the expression

$$\chi'(\mathrm{T}) = -\frac{N}{H} \cdot \frac{\sum_i \left(\frac{\partial E_i}{\partial H}\right) \exp\left(-E_i/kT\right)}{\sum_i \exp\left(-E_i/kT\right)} \Big/ n + \frac{C}{T} + K \qquad (1)$$

by minimization of

$$\sum_j \frac{[\chi_{obs}(T_j) - \chi'(T_j)]^2}{\sigma^2\left(\chi(T_j)\right) + \left(\frac{\partial \chi_{obs}}{\partial T}(T_j)\right)^2 \sigma^2(T_j)} \qquad (2)$$

Here, χ_{obs} is the measured molar susceptibility per chromium atom, corrected for diamagnetic contributions using Pascal constants, and n is the number of chromium atoms in the polynuclear complex being studied. The E_i in (1) are the energies of the components of the ground state manifold of the complex as obtained by diagonalization of the isotropic Heisenberg-type model Hamiltonian

$$\hat{\mathcal{H}} = \sum_{k<l}^{n} \{J_{kl}\hat{\mathbf{S}}_k \cdot \hat{\mathbf{S}}_l + j_{kl}(\hat{\mathbf{S}}_k \cdot \hat{\mathbf{S}}_l)^2\} + \beta g\, \mathbf{H} \cdot \hat{\mathbf{S}} \qquad (3)$$

The adjustable parameters are g, C, K, the bilinear coupling constants J_{kl}, and the biquadratic coupling constants j_{kl}. The estimated standard deviations used in (2) are reported elsewhere.[15]

The fitting was accomplished using a new

general computer program. The central part of this program is a subroutine which can diagonalize $\hat{\mathcal{H}}$ in (3) for an arbitrary spin system (that is, an arbitrary number of spins with no restrictions on the values S_k) with arbitrary values of the J_{kl}'s and the j_{kl}'s, the only limitation being computer capacity. The basis for this diagonalization is a formula giving the various types of matrix elements of a general operator $\hat{\mathbf{S}}_k \cdot \hat{\mathbf{S}}_l$ with $k<l$ in a basis defined by successive coupling of the spins $\mathbf{S}_1,\mathbf{S}_2,\mathbf{S}_3,\ldots$:

In eqn. (4), the various symbols have the following meaning: The numbers S_{12}, S_{123}, *etc.*, are intermediary spin quantum numbers defined by the successive coupling scheme

$\mathbf{S}_{12}=\mathbf{S}_1+\mathbf{S}_2$, $\mathbf{S}_{123}=\mathbf{S}_{12}+\mathbf{S}_3$, *etc.*

The number S is the total spin and M a magnetic quantum number corresponding to S. All δ's with two arguments are Kronecker deltas. The braces denote 6-j symbols.[16–18]

Note that any operator $\hat{\mathbf{S}}_k \cdot \hat{\mathbf{S}}_l$, and thus $\hat{\mathcal{H}}$ as a whole, is diagonal in S and M.

The matrices of the biquadratic terms in (3) were calculated simply by squaring the matrices of the corresponding bilinear terms.

Formula (4) was derived by using Wigner-Racah algebra for the rotation group, *i.e.*, the "irreducible tensor methods" developed by Fano and Racah [19] and also exposed in Ref. 18. During this work, we became aware that equivalent formulae were derived many years ago by Thaddeus *et al.*;[20] however, (4) is more readily applicable for our purpose. In the program, the 6-j symbols appearing in (4) are evaluated by the explicit formulae (2.22)–(2.25) in Ref. 16.

Any desired subset of the total set $\{J_{12}, J_{13},\ldots,J_{23},J_{24},\ldots,j_{12},j_{13},\ldots,j_{23},j_{24},\ldots,g,C,K\}$ of parameters can be fitted with arbitrary linear constraints on the J_{kl}'s and on the j_{kl}'s. The

$$\langle((\ldots((S_1S_2)S_{12}S_3)S_{123}\ldots)S_{12\ldots n-1}S_n)SM|\hat{\mathbf{S}}_k\cdot\hat{\mathbf{S}}_l|((\ldots((S_1S_2)S'_{12}S_3)S'_{123}\ldots)S'_{12\ldots n-1}S_n)S'M'\rangle$$

$$=\hbar^2\delta\sqrt{\rho}\,(-1)^{\phi}\;\frac{1}{1+2S_1\delta(k,1)}\cdot F_{1<l-k}F_{1<k}\begin{Bmatrix} S_{1\ldots l-1} & S'_{1\ldots l-1} & 1\\ S_l & S_l & S_{1\ldots l}\end{Bmatrix}, \qquad (4)$$

where

$$\delta=\begin{cases}\delta(M,M')\delta(S,S')\delta(S_{12\ldots n-1},S'_{12\ldots n-1})\ldots\delta(S_{1\ldots l},S'_{1\ldots l})\delta(S_{1\ldots k-1},S'_{1\ldots k-1})\ldots\delta(S_{12},S'_{12}) & \\ \qquad\qquad\qquad\qquad\qquad\qquad\qquad\qquad\qquad\qquad\qquad\qquad \text{if } 1<k \text{ and } l<n\\ \delta(M,M')\delta(S,S')\delta(S_{12\ldots n-1},S'_{12\ldots n-1})\ldots\delta(S_{1\ldots l},S'_{1\ldots l}) \text{ if } 1=k \text{ and } l<n\\ \delta(M,M')\delta(S,S')\delta(S_{1\ldots k-1},S'_{1\ldots k-1})\ldots\delta(S_{12},S'_{12}) \quad \text{if } 1<k \text{ and } l=n\\ \delta(M,M')\delta(S,S') \quad \text{if } 1=k \text{ and } l=n\end{cases};$$

$$\phi=l+(S_l+\ldots+S_k)+(S_{1\ldots l}+\ldots+S_{1\ldots k})+(S'_{1\ldots l}+\ldots+S'_{1\ldots k+1})$$
$$+(S'_{1\ldots l-1}-S_{1\ldots l-1})-S_1\cdot\delta(k,1)+(-k+S_{1\ldots k}+S_{1\ldots k-1})(1-\delta(k,1));$$

$$\rho=S_k(S_k+1)(2S_k+1)S_l(S_l+1)(2S_l+1)$$
$$\times(2S_{1\ldots l-1}+1)\ldots(2S_{1\ldots k}+1)(2\,S'_{1\ldots l-1}+1)\ldots(2S'_{1\ldots k}+1);$$

$$F_{1<l-k}=\begin{Bmatrix} S_{1\ldots l-1} & S'_{1\ldots l-1} & 1\\ S'_{1\ldots l-2} & S_{1\ldots l-2} & S_{l-1}\end{Bmatrix}\ldots\begin{Bmatrix} S_{1\ldots k+1} & S'_{1\ldots k+1} & 1\\ S'_{1\ldots k} & S_{1\ldots k} & S_{k+1}\end{Bmatrix} \text{ if } 1<l-k$$

$$\text{and}=1 \text{ if } l-k=1;$$

$$F_{1<k}=\begin{Bmatrix} S_{1\ldots k} & S'_{1\ldots k} & 1\\ S_k & S_k & S_{1\ldots k-1}\end{Bmatrix} \text{ if } 1<k \text{ and } =1 \text{ if } k=1.$$

Scheme 1. Eqn. (4).

minimization is carried out using a statistical subroutine developed previously in this laboratory by Dr. Ole Mønsted.

The energy subroutine also exists as a separate program, which was used in determining the zero-field eigenvalues of $\hat{\mathcal{H}}$ defined in (3) for the parameter values obtained by the fitting procedure. The programs are written in Algol 6 and are available on request. For other applications of the energy program, see Ref. 21.

Güdel *et al.* have previously given formulae corresponding to (4) for various specific 4-center systems[22–24] (using sometimes a different coupling scheme[22]) and have used these in connection with fitting of susceptibility data.[22,23,25]

For polynuclear complexes with certain symmetries and thus certain relations between the coupling constants, *explicit* expressions for the eigenvalues of the bilinear part of the Hamiltonian in (3) may be derived.[26–30] This category

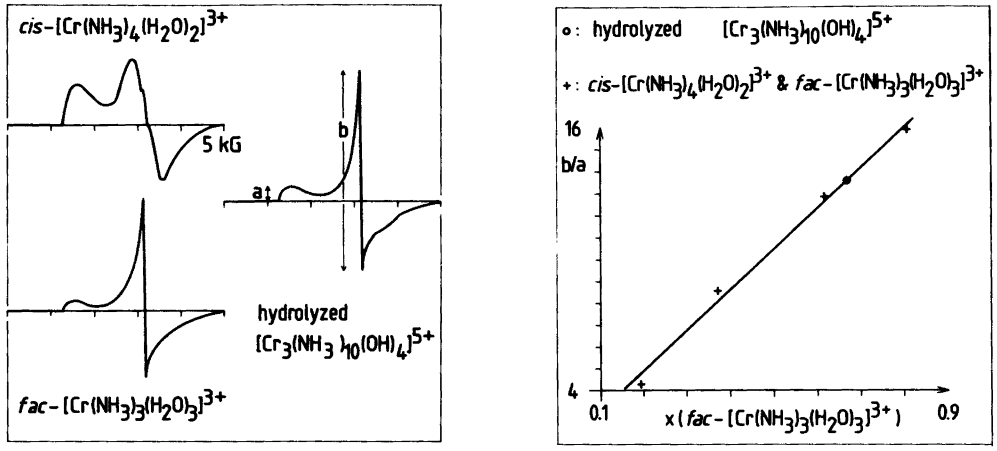

Fig. 1. Left: First derivative ESR spectra (frozen glasses) for the analysis of the hydrolysis products of $[Cr_3(NH_3)_{10}(OH)_4]^{5+}$. The ratio, *b/a*, for different mixtures of the two mononuclear species determined the *fac*-triaquatriammine/*cis*-diaquatetraammine ratio to 2 (*right*).

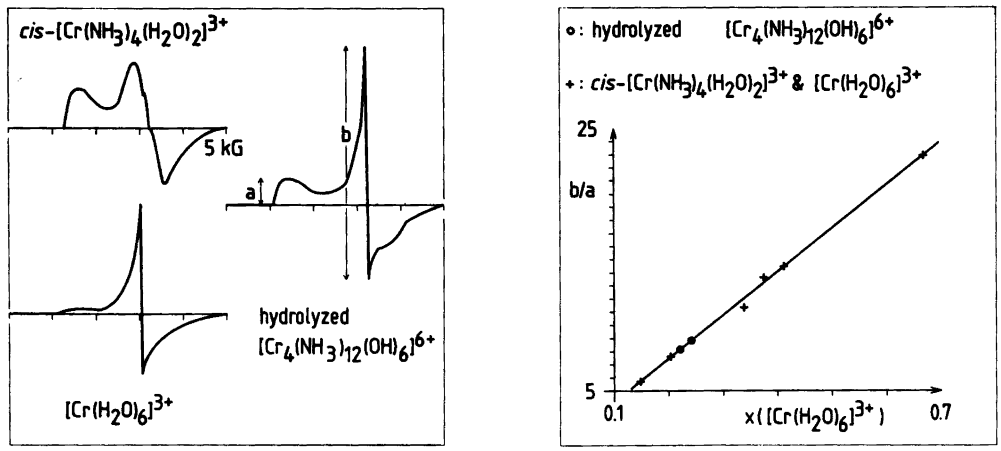

Fig. 2. Left: First derivative ESR spectra (frozen glasses) for the analysis of the hydrolysis products of $[Cr\{(OH)_2Cr(NH_3)_4\}_3]^{6+}$. The ratio, *b/a*, for different mixtures of the two mononuclear species determined the *cis*-diaquatetraammine/hexaaqua ratio to 3 (*right*).

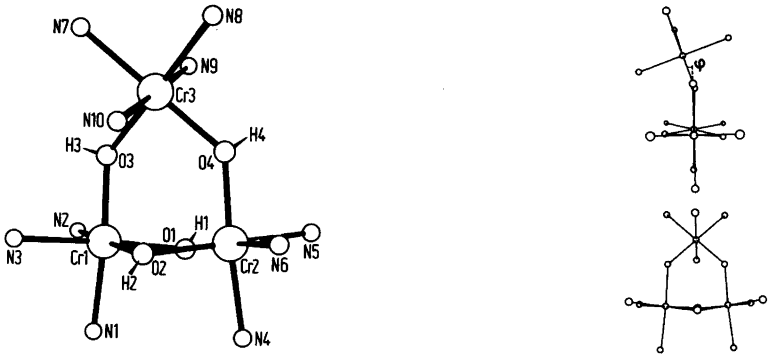

Fig. 3. Left: Numbered ORTEP-drawing of the $[Cr_3(NH_3)_{10}(OH)_4]^{5+}$ ion with arbitrary atomic radii and indicated positions of the four OH-hydrogen atoms. *Right:* Computer-drawn sketches of the ion for further illustration of the structure and the symmetry: The point group is C_s within the standard deviation of the atomic positions.

includes the two four-center systems represented in the present paper (if $J_{13}=J_{14}=J_{23}=J_{24}$ is assumed for the rhodoso ion (*cf.* Fig. 6) and $J_{12}=J_{13}=J_{14}$ and $J_{23}=J_{24}=J_{34}$ are assumed for the $[Cr\{(OH)_2Cr(NH_3)_4\}_3]^{6+}$ ion).[23,30]

For a general 3-center system Griffith has given explicit formulae for the matrix elements of the full exchange Hamiltonian of (3) in the same basis as we used in (4), derived by the same method.[29,31]

RESULTS AND DISCUSSION

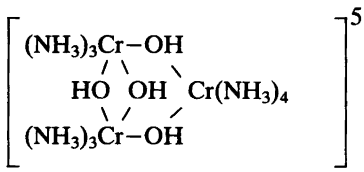

This ion, di-μ-hydroxo-μ-{*cis*-[tetraamminedihydroxochromium(III)]}-bis{*fac*-[triamminechromium(III)]}, was isolated from the first, red polynuclear ion-exchange band as the iodide and bromide. Hydrolysis of the bromide with 70 % perchloric acid gave *cis*-$[Cr(NH_3)_4(H_2O)_2]^{3+}$ and *fac*-$[Cr(NH_3)_3(H_2O)_3]^{3+}$ in a 1:2 ratio (see Fig. 1).

The X-ray structure analysis (see experimental section) of the bromide shows that the complex is built very similar to one of the very few other known trinuclear chromium(III) complexes, namely the $[Cr_3(C_6H_{15}N_3)_3(OH)_5]^{4+}$ ion[32] ($C_6H_{15}N_3$=1,4,7-triazacyclononane) in having a tilted octahedron as a "bridge" on top of a diol (=di-μ-hydroxo) moiety. The inclination, ϕ (see Fig. 3), is 21° in our case (O2–N10=2.930(15) Å) and 37° in the latter compound. Intramolecular bond distances and angles between Cr, N, and O atoms are in accordance with those found in other polynuclear chromium(III) ammines.[33,34] The OH bridges 1–4 are hydrogen bonded to Br4, Br5, Br3, and O5 of a water of crystallization, respectively (see Table 3) and all the bromide ions are involved in a three-dimensional

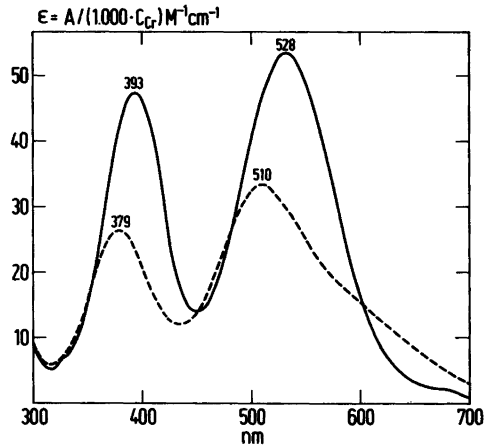

Fig. 4. Optical spectra of $[Cr_3(NH_3)_{10}(OH)_4]Br_5 \cdot 3H_2O$(——) and $[Cr\{(OH)_2Cr(NH_3)_4\}_3]Br_6 \cdot nH_2O$(– – –) in water. The spectra did not change within 10–15 min and showed only small changes after the addition of acid or base.

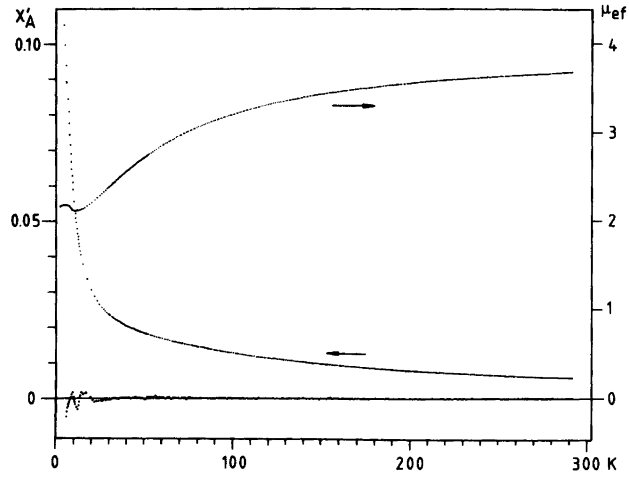

Fig. 5. Magnetic susceptibility per chromium (left scale, cgs units) and effective moment (right scale, Bohr magnetons) of $[Cr_3(NH_3)_{10}(OH)_4]Br_5 \cdot 3H_2O$. The lower, almost random, distribution of dots around the abscissa indicates the corresponding values of $(\chi_{obs}-\chi_{calc})\times 25$, where χ_{calc} refers to the parameters of minimum I in Table 5.

network with several 3.3–3.5 Å contact distances to nitrogen and oxygen from water of crystallization.

The temperature variations of the susceptibility and of the effective moment of the bromide salt are shown in Fig. 5. The susceptibility data were fitted to a model based on (1) and (3) with a variable g-factor and with the restrictions $J_{13}=J_{23}$ and $j_{13}=j_{23}=0$ on the exchange interaction parameters defined in Fig. 6. (It proved impossible to fit a model including j_{12} *as well as* $j_{13}=j_{23}$.) This model seemed reasonable in view of the distances and angles reported in Table 3 for the monohydroxo bridges, a rough estimate of the uncertainty in the unrefined hydrogen positions leading to estimated standard deviations on the out-of-bridge-plane angles of these atoms of around 10°. (Later calculations indicate that a fit with three J-parameters would be unsatisfactory because of very high correlations between the parameters.)

The resulting parameter values are given in Table 5. Depending on the choices of initial parameters, we found two minima of (2), one with $J_{13}=J_{23}>J_{12}$, the other with $J_{13}=J_{23}<J_{12}$. The qualities of the two fits are almost equal if

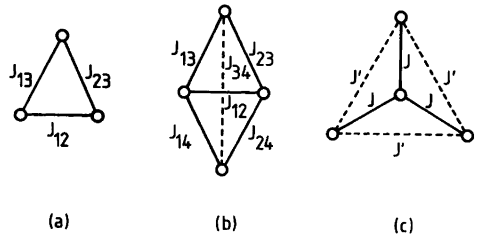

Fig. 6. Definition of J parameters in tri- and tetranuclear complexes. The parameters j are defined correspondingly.

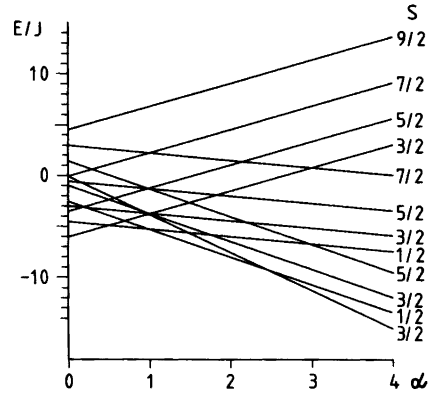

Fig. 7. Energy diagram for a trinuclear cluster with $S_i=3/2$ corresponding to $\hat{\mathcal{H}}=J(\alpha\ \hat{\mathbf{S}}_1 \cdot \hat{\mathbf{S}}_2+\hat{\mathbf{S}}_1 \cdot \hat{\mathbf{S}}_3+\hat{\mathbf{S}}_2 \cdot \hat{\mathbf{S}}_3)$; referring to Fig. 6a, we have put $J_{13}=J_{23}=J$ and $J_{12}/J=\alpha$.

Table 4. X-Ray powder data. The dithionates were prepared by methathesis from the bromide (see experimental section) and the chloride,[36] respectively. Rhodoso chloride was prepared as described in the experimental section.

$[Cr\{(OH)_2Cr(NH_3)_4\}_3](S_2O_6)_3 \cdot aq$				$[Co\{(OH)_2Co(NH_3)_4\}_3](S_2O_6)_3 \cdot aq$			Rhodoso chloride tetrahydrate			
hkl	Int.	d_{obs}(Å)	d_{calc}(Å)	Int.	d_{obs}(Å)	d_{calc}(Å)	*hkl*	Int.	d_{obs}(Å)	d_{calc}(Å)
002	vw	9.96	9.95				011	m	9.12	9.11
200	vw	9.19	9.16	vw	8.34	8.33	$\bar{1}11$	mw	7.52	7.51
$\bar{1}11$	vw	8.12	8.12	w	7.90	7.91	021	vw	6.85	6.85
111	w	7.72	7.71	w	7.47	7.47	$\bar{1}02$	w	6.70	6.69
$\bar{2}02$	vw	7.31	7.31	vw	7.24	7.25	100	w	6.33	6.34
202	w	6.28	6.28	w	6.10	6.11	$\bar{1}21$	vw	6.09	6.09
103	vw	5.949	5.955	w	6.23	6.25	110	w	5.982	5.978
$\bar{2}12$	w	5.856	5.853	vw	5.751	5.749	120	vw	5.182	5.182
301	vvw	5.600	5.607				041	vw	4.144	4.141
$\bar{3}13$	vw	5.451	5.446				$\bar{2}12$	w	4.025	4.026
113				vw	5.219	5.210	140	w	3.669	3.670
212				vw	5.137	5.131	$\bar{2}23$	vw	3.595	3.595
$\bar{3}11$	vw	5.174	5.176	m	4.831	4.831	131	vw	3.516	3.517
020	s	4.880	4.880	s	4.723	4.723	$\bar{2}21$	vvw	3.483	3.482
311				vw	4.532	4.534	051	vvw	3.410	3.409
120	vw	4.716	4.716			4.544	$\bar{1}04$	vw	3.306	3.305
400	vw	4.582	4.583				$\bar{1}14$	vw	3.249	3.251
014	w	4.435	4.432				$\bar{1}43$	vvw	3.204	3.205
$\bar{1}15$				w	3.981	3.980	$\bar{1}52$	vvw	3.170	3.171
221	mw	4.146	4.149			3.975				
410			4.148				Indexing based on			
$\bar{2}15$				vw	3.806	3.804				
222	vvw	3.852	3.854	vw	3.734	3.737	a= 8.2$_7$ Å $\alpha=\gamma$= 90.00°			
123	vvw	3.776	3.775				b=18.0$_1$ Å β=130.$_0$°			
$\bar{3}23$	w	3.451	3.449	w	3.377	3.377	c=13.7$_9$ Å			
Indexing based on							E.Bang[39]:			
a=18.5$_4$ Å $\alpha=\gamma$=90.00°				a=16.9$_2$ Å $\alpha=\gamma$= 90.00°			a= 8.26 Å $\alpha=\gamma$= 90.00°			
b= 9.7$_6$ Å β=98.$_7$°				b= 9.4$_5$ Å β=100.$_1$°			b=17.95 Å β=130.0°			
c=20.1$_3$ Å				c=22.0$_3$ Å			c=13.74 Å			
Figure of merit:[46] M_{19}=12				M_{16}=9						

Table 5. Parameters for $[Cr_3(NH_3)_{10}(OH)_4]Br_5 \cdot 3H_2O$ (*cf.* Fig. 6a) derived from magnetic susceptibility data in the temperature range 4–290 K.

	I	II
g	1.982(1)	1.983(6)
J_{12}/cm^{-1}	7.90(1)	18.7(3)
$J_{13}=J_{23}$/cm^{-1}	18.7(1)	4.3(1)
j_{12}/cm^{-1}	0.09(2)	0.24(9)
f^a	383	383
v/f^b	1.4	2.6

[a] Degrees of freedom. [b] Variance per degree of freedom.

evaluated by their variances per degree of freedom. The first set exhibits a much sharper minimum. Both sets of parameters correspond to a quartet ground state having a doublet as the nearest excited state at *ca.* 5 cm^{-1}. This is in agreement with the interval of decreasing moment with increasing temperature. Since $j_{12} \ll J_{12}$ in both cases, the energy diagram in Fig. 7 may be used to roughly represent the energy spectra of the system for the obtained values of the ratio J_{12}/J_{23}.

The temperature variations of the ESR spectra of powdered samples at low temperatures are illustrated in Fig. 8. The sample was not magneti-

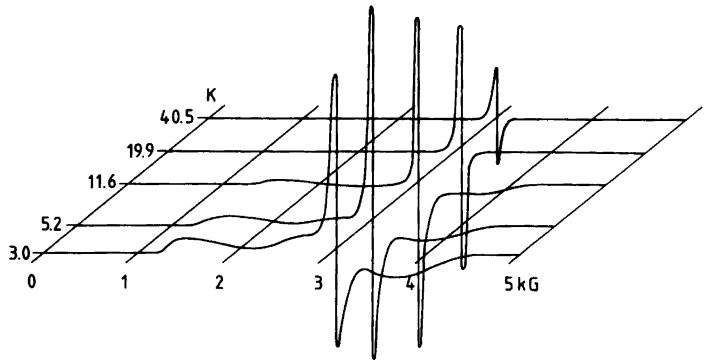

Fig. 8. ESR spectra of powdered samples of $[Cr_3(NH_3)_{10}(OH)_4]Br_5 \cdot 3H_2O$ *vs.* temperature recorded at 9.10 GHz.

cally diluted since a suitable diamagnetic host lattice is hitherto unknown. In spite of that, however, the linewidths are not excessive, thus indicating fairly small intermolecular interactions. The spectra in the range 3.0–41 K show competing signals from an isotropic doublet transition corresponding to g around 1.98 and an anisotropic quartet spectrum, the latter gaining intensity with decreasing temperature. Considering the large span of the quartet spectrum it is obvious that the integrated intensity of the quartet signal is much bigger than that of the doublet. This is consistent with the conclusions drawn above from the susceptibility measurements. The quartet spectrum is rather similar to the spectrum of *cis*-$[Cr(NH_3)_4(H_2O)_2]^{3+}$ as seen from Fig. 1.

The two-center exchange parameters can be compared with the data for dinuclear species *via* the semi-empirical GHP model already available.[4] The di-μ-hydroxo fragment containing Cr1 and Cr2 has Cr–O distances, r, Cr–O–Cr angles, ϕ, and out-of-bridge-plane angles for the hydrogen atoms, θ, comparable to those found in similar real dimers. The individual r and ϕ values found in the trimer differ very little. The values of the θ's differ substantially, however. In order to calculate the value of J_{12} according to the GHP-model, we have calculated the contribution of each exchange path for itself using average values for r and ϕ and individual θ values. The resulting model value of J_{12} was 8 cm^{-1} with an estimated standard deviation of 3 cm^{-1} arising from the estimated uncertainties on the hydrogen positions mentioned above.

As for the mono-hydroxo bridges, sufficient material is at present not available for corresponding dimers to allow for a proper model value to be proposed. It is tempting, however, to use the structural and magnetic results for *cis*-$[(NH_3)_4(OH)Cr(OH)Cr(NH_3)_5](S_2O_6)_2 \cdot 3H_2O$ for a comparison.[33] The r and θ values of the two fragments of the trimer differ about or less than one standard deviation from the values found in this mono-μ-hydroxo complex. Only the ϕ values differ (142.8° in the dimer *vs.* 134.5° in the trimer). The value of J in the dimer is 21 cm^{-1}.

The above model considerations agree well with the parameters corresponding to minimum (I) of Table 5 if J_{12} is interpreted as the di-hydroxo-bridge coupling constant. The values $J_{13}=J_{23}=19$ cm^{-1} then correspond to the mono-hydroxo bridges and conform, when compared with the above value of 21 cm^{-1}, to the general

Table 6. Parameters for $[Cr\{(OH)_2Cr(NH_3)_4\}_3]Br_6.nH_2O$ [a] (*cf.* Fig. 6c) derived from magnetic susceptibility data in the temperature range 4–273 K.

g	2.001(2)	1.993(3)
J/cm^{-1}	10.9(1)	9.3(1)
J'/cm^{-1}	0.98(2)	–
j/cm^{-1}	−0.42(5)	–
f [b]	395	397
v/f [c]	1.9	31.9

[a] n was determined from chromium analyses prior to measurements. [b] Degrees of freedom. [c] Variance per degree of freedom.

Table 7. Parameters for $[Cr_4(NH_3)_{12}(OH)_6]Cl_6 \cdot 4H_2O$ (rhodoso) (*cf.* Fig. 6b) derived from magnetic susceptibility data. The parameters $g=1.98$ and $C=0$ were fixed in all cases. The results are arranged according to increasing v/f[b] value. Results for which $v/f>600$ were excluded.

J_{12}/cm^{-1}	32.7(3)	24.4(1)	23.9(1)	30.4(4)	27.3(1)	29(1)	29(2)
$J_{13}=J_{24}/cm^{-1}$	|	|	22.27(4)	|	|	|	|
	19.7(1)	19.12(1)		18.21(3)	19.02(3)	18.4(3)	19(1)
$J_{14}=J_{23}/cm^{-1}$	|	|	13.8(1)	|	|	|	|
J_{34}/cm^{-1}	–	–	–	–	–	–	−1(3)
j_{12}/cm^{-1}	0.9(1)	−2.1(1)	−3.5(1)	−0.8(1)	−1.80(1)	–	–
$j_{13}=j_{23}=j_{24}=j_{14}/cm^{-1}$	0.36(4)	0.61(1)	–	–	–	–	–
K	$2.6(4)\cdot10^{-4}$	–	–	–	–	–	–
f[a]	359	394	925	926	395	396	395
v/f[b]	1.64	2.29	4.26	17.3	60.4	506	507
$T_{min}-T_{max}$[c]/K	10.4–100	3.0–93	4.3–191	4.3–191	3.0–93	3.0–100	3.0–93
E/cm^{-1}[d]	+29.1	−2.3	−3.1	+15	−2.2	+13.3	+14

[a] Degrees of freedom. [b] Variance per degree of freedom. [c] Temperature interval of data subset. [d] Calculated energy of the lowest *singlet* relative to the lowest *triplet* state. The fits in the first and the fourth column have a *quintet* between the triplet and the singlet at about one-half the singlet energy.

observation that the coupling constant decreases with decreasing ϕ in mono-hydroxo-bridged dimers.

Minimum (II) of Table 5 agrees poorly with the model parameter values if we again let J_{12} correspond to the dihydroxo bridge. However, minimum (I) as well as (II) may also be interpreted as involving two different mono-hydroxo-bridge couplings, one of which is then equal to the di-hydroxo-bridge coupling.

The reader may further wish to compare the parameter sets for the present "3/4 rhodoso" complex with some of those for the full rhodoso complex reported in Table 7; we do not, however, think that the available data warrant an elaborate discussion of this comparison.

As a conclusion, we can say that the magnetic behaviour of this trinuclear complex can be described in terms of sums of two-center interactions. The parameters obtained from minimum (I) of (2) are in good agreement with interactions previously found for dinuclear complexes having r, ϕ, and θ values similar to the two-center fragments in the trimer.

$[Cr\{(OH)_2Cr(NH_3)_4\}_3]^{6+}$

This ion, tris{di-μ-hydroxo-tetraamminechromium(III)}-chromium(III), was found in the second, violet ion-exchange band and was isolated as the iodide and bromide a.o. salts. It is the chromium ammonia analogue of Werner's brown salt of cobalt(III) and ethylenediamine,[35] and its identification is based on the following three observations:

Hydrolysis of the bromide with 70 % perchloric acid gave *cis*-$[Cr(NH_3)_4(H_2O)_2]^{3+}$ and $[Cr(H_2O)_6]^{3+}$ in a 3:1 ratio (see Fig. 2).

The X-ray powder photographs of the dithionates of the chromium compound and of $[Co\{(OH)_2Co(NH_3)_4\}_3]^{6+}$ (Ref. 36) show that these two salts may have structural similarities (see Table 4). Single crystal Weissenberg photographs of the chromium salt confirm the unit cell dimensions of Table 4.

The visible spectrum of the tetranuclear chromium(III) compound is shown in Fig. 4, together with that of the above-mentioned trinuclear complex. The spectrum of the former is rather similar to that of $[Cr\{(OH)_2Cr\ en_2\}_3]^{6+}$ (Ref. 3), which also shows a characteristic irregularity around 600 nm.

Thus, although it has not yet been possible to grow single crystals suited for X-ray diffraction for confirmation of the structure, there is little doubt that the compound is the analogue of Werner's brown salt.

The temperature variations of the susceptibility and of the effective moment of the bromide salt are seen in Fig. 9. These data were fitted to (1) using the Hamiltonian (3) by minimization of (2) and including a variable g-factor and the exchange parameters J, j, and J' defined in Fig. 6. The resulting set of parameters is shown in Table 6. By omission of j and J' the variance per degree

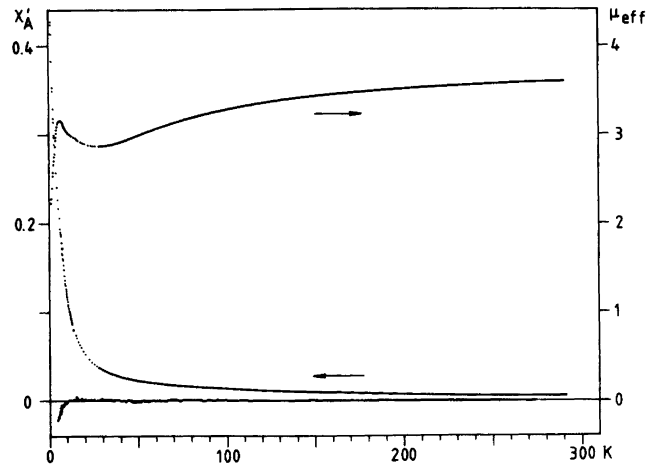

Fig. 9. Magnetic susceptibility per chromium (left scale, cgs units) and effective moment (right scale, Bohr magnetons) of $[Cr\{(OH)_2Cr(NH_3)_4\}_3]Br_6.aq$. The lower distribution of dots around the abscissa indicates the corresponding values of $(\chi_{obs}-\chi_{calc})\times 25$, where χ_{calc} refers to the parameters of the left column in Table 6.

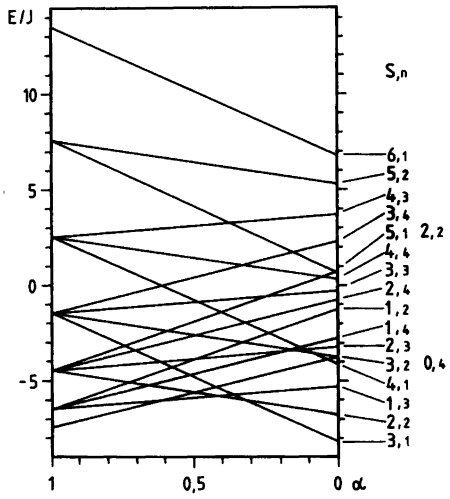

Fig. 10. Energy diagram for a tetranuclear cluster with $S_i=3/2$ corresponding to

$$\hat{\mathcal{H}}=J\{\hat{S}_1\cdot\hat{S}_2+\hat{S}_1\cdot\hat{S}_3+\hat{S}_1\cdot\hat{S}_4+\alpha(\hat{S}_2\cdot\hat{S}_3+\hat{S}_3\cdot\hat{S}_4+\hat{S}_2\cdot\hat{S}_4)\};$$

referring to Fig. 6c, we have put $J'/J=\alpha$. The number n indicates the number of spin multiplets with spin S.

of freedom of the fits increased significantly. A fit with four exhange parameters including j' was very good from a statistical point of view but led to so ridiculous J/j and J'/j' values that the results will not be reproduced here. Even the simple two-parameter model with only one exchange parameter, J, gives a rather good fit to the experiments.

According to all models we have tried, the ground state is a septet, followed by two degenerate quintet states with zero-field energies of *ca.* 1.5 J and three nearly degenerate triplet states with zero-field energies of *ca.* 3 J. These energy expressions are valid exactly in the exchange model including only J. The complete energy diagram for the ground state manifold when $j=0$ is shown in Fig. 10. The ground state can have $S=0$, 1, 2, or 3 depending on J'/J.

The ESR spectrum of a powdered sample was very complex and continued to gain intensity with decreasing temperature, even at 2.9 K, our lower limit. This is in agreement with the conclusion drawn from susceptibility data that at this temperature the only state populated should be the septet ground state. No further interpretation of the spectrum can be given.

The nearest-neighbour interaction, $J\approx 10$ cm^{-1}, cannot in detail be compared with data for dinuclear species since accurate crystallographic

information is missing for the tetramer. The J value is as expected for a di-μ-hydroxo-bis[tetraamminechromium(III)] ion having an almost planar bridging system (including the hydrogens) and normal Cr–O distances.[4] For the tetranuclear ethylenediamine analogue, $J \approx 18$ cm^{-1} was found.[23] This is exactly as expected for a corresponding dinuclear fragment with an almost planar bridging system.[4] The di-μ-hydroxo complexes with ethylenediamine generally exhibit larger coupling constants than their ammonia analogues with similar angles in the bridging system, mainly because of shorter Cr–O distances. The next-nearest-neighbour interaction, J', was found to be small which is consistent with the long superexchange pathways.

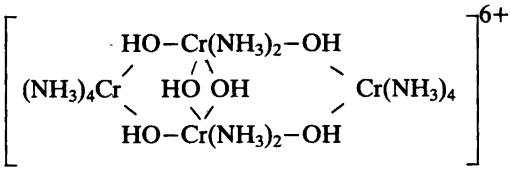

This ion, di-μ-hydroxo-bis-μ-{*cis*-[tetraamminedihydroxochromium(III)]}-bis{*cis*-[diamminechromium(III)]}, the rhodoso, was first prepared by Jørgensen.[37] The synthesis presented here is faster and more reliable and gives the bromide in a good yield.

Hydrolysis with 70 % perchloric acid is not possible due to low solubility. Treatment with concentrated hydrochloric acid, however, gives almost quantitatively *cis*-$[Cr(NH_3)_4(H_2O)Cl]Cl_2$ and $[Cr(NH_3)_2(H_2O)_2Cl_2]Cl$, the latter having *cis*-configuration with respect to NH_3 and *trans*-configuration with respect to Cl.[38]

X-Ray powder photographs of the chloride (Table 4) and the bromide confirm that these are salts of Jørgensen's rhodoso. Single crystal X-ray diffraction has shown that the structure is as indicated above and on Fig. 12, with an eight-membered ring of alternating Cr and O atoms and with an inclination $\phi \approx 14°$(see Fig. 3).[39,40,41] The ethylenediamine analogue[3,42] seems to have a similar structure.[43]

The temperature variations of the susceptibility and of the effective moment of the chloride salt are shown in Fig. 11. X-Ray powder data as shown in Table 4 show that our samples were identical to those used for structural determinations by E. Bang[39,41]; one of the samples used for magnetic measurements was, in fact, *the same* as that used for single crystal X-ray diffraction in Ref. 41.

The susceptibility data were fitted to several different models based on (3), using various subsets of three independent data sets. The relevant exchange parameters are defined in Fig. 6. Initially we included the g-factor as a variable,

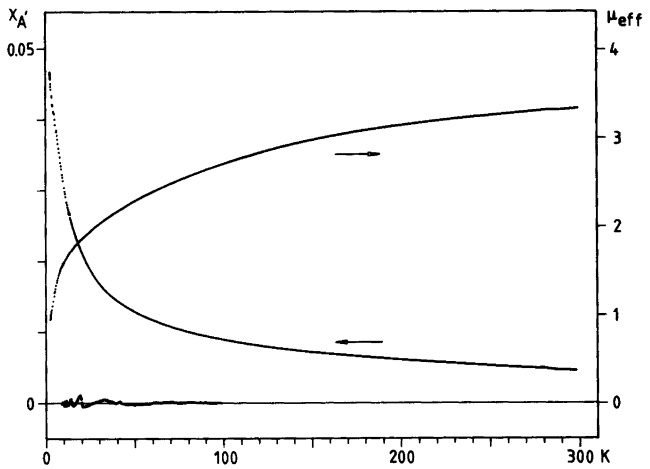

Fig. 11. Magnetic susceptibility per chromium (left scale, cgs units) and effective moment (right scale, Bohr magnetons) of $[Cr_4(NH_3)_{12}(OH)_6]Cl_6 \cdot 4H_2O$ (rhodoso). The lower, almost random, distribution of dots around the abscissa indicates the corresponding values of $(\chi_{obs}-\chi_{calc})\times 25$, where χ_{calc} refers to the parameters of the first column to the left in Table 7.

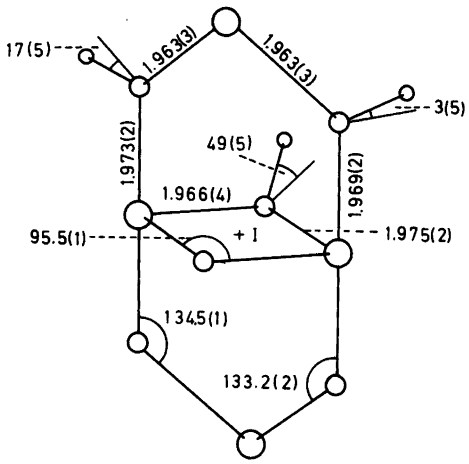

Fig. 12. The rhomboid bridging system of the tetranuclear cation in $[Cr_4(NH_3)_{12}(OH)_6]Cl_6 \cdot 4H_2O$ (rhodoso chloride) according to Ref. 41. Bond lengths in Å, bond angles in degrees. There is a crystallographic inversion centre at I.

but it soon became obvious that all parameters came out with unrealistic values unless g was fixed to be 1.98. Another early observation was that all fits exhibited a low-lying or even ground spin triplet. Considering that such a triplet may have quite large zero-field splittings [which may result in a smaller contribution to the effective moment at low temperatures than expected from (1) when using (3)], we omitted data below 4.3 or 10.4 K in some of the data subsets used. Also, in order to get some insight in the variation of the resultant parameters with temperature, the upper temperature limits were variously chosen at around 90, 190 or 270 K. No evidence for temperature dependences were found. A small selection of typical results is given in Table 7.

The coupling constants exhibit rather small variations among the different models whereas the variations of the calculated energy spectrum were dramatic as seen even for the two lowest states. An idea of the complexity of the energy diagram for the ground manifold can be obtained from Fig. 4 in Ref. 45. Those of our fittings which give a singlet ground state lead to a singlet-triplet splitting of *ca.* 3 cm^{-1}, in fair agreement with the results obtained by Güdel *et al.*[22,25,44,45] for a corresponding deuterated complex. H. Güdel has pointed out (personal communication) that the rhodoso chloride crystals used in his group may belong to a modification sufficiently different from ours to have different magnetic properties.

Single crystal and powder ESR spectra in the temperature range 3.0–50 K were measured on non-diluted samples, since a diamagnetic host was not available. The most characteristic feature among the multitude of rather narrow lines was an almost isotropic transition with varying position in the range 10–15 mT at the frequency of 9.09 GHz. Judging from the double integral of the first derivative spectrum its intensity continued to increase rapidly with decreasing temperature around 3.0 K. The rest of the spectrum was very anisotropic and showed strongly decreasing intensity with temperature at the lower end of the temperature interval. The almost isotropic line is therefore assigned as a "zero-field transition" among the states of the lowest triplet and the others as transitions within the nearest other states which always included a quintet and a triplet.

According to these ESR results, the ground spin multiplet should either be a triplet or a singlet with an excited triplet at *ca.* 1 cm^{-1}. The itensity of the "zero-field" ESR transition, however, varied more strongly around 3 K than expected from calculated population differences. This might indicate that temperature variations of relaxation times play a rôle with some importance for the validity of conclusions drawn from ESR data.

The two-center exchange interactions can now be compared with improved structural information based on low temperature X-ray data, including refinement of all hydrogen positions, as very recently obtained by E. Bang.[41] A sketch of the rhomboid bridging system is given in Fig. 12. The couplings *via* the mono-μ-hydroxo bridges are in fair agreement with the results found for their corresponding dimeric fragments as discussed above for $[Cr_3(NH_3)_{10}(OH)_4]Br_5 \cdot 3H_2O$. The coupling constant for the di-μ-hydroxo fragment is calculated *via* the GHP-model to be 9(4) cm^{-1}, based on data from Fig. 12 using average values of r. The results of the data fittings are at least twice as large, a discrepancy not explained by uncertainties of the atomic positions. An explanation might be that the GHP-model does not enable us to take into account the extra exchange pathways connecting Cr1 and Cr2 in the rhodoso system, namely those going via Cr3 and Cr4

[numbering the Cr atoms in accordance with Fig. 6 (b)].

Acknowledgements. Dr. T. Berg has contributed to the work on the synthesis and hydrolysis of rhodoso, and the authors are grateful to Dr. S. Larsen and F. Hansen for their valuable help with the X-ray work and to K.M. Nielsen, K. Jørgensen and S. Kallesøe for their contributions to the synthetic and analytical work and to the collection of magnetic data, respectively. We thank Dr. E. Bang for permission to publish Fig. 12 prior to publication of Ref. 41. This research was supported by the Danish Natural Science Research Council through grants Nos. 511–742, 511–3993, 511–10516 (to E.P.) and grants Nos. 511–20608, 11–2205, and 11–3296 (to T.D.).

REFERENCES

1. Andersen, P., Berg, T. and Jacobsen, J. *Acta Chem. Scand. A 29* (1975) 381.
2. Andersen, P., Berg, T. and Jacobsen, J. *Acta Chem. Scand. A 29* (1975) 599.
3. Andersen, P. and Berg, T. *Acta Chem. Scand. A 32* (1978) 989.
4. Glerup, J., Hodgson, D. J. and Pedersen, E. *Acta Chem. Scand. A 37* (1983) 161.
5. Josephsen, J. and Pedersen, E. *Inorg. Chem. 16* (1977) 2534 and references therein.
6. Andersen, P., Nielsen, K. M. and Petersen, A. *Acta Chem. Scand. A 38* (1984). *In press.*
7. Springborg, J. and Schäffer, C. E. *Inorg. Synth. 18* (1978) 75.
8. Coppens, P., Leiserowitz, L. and Rabinovich, D. *Acta Crystallogr. 18* (1965) 1035.
9. Lehnert, P. G. *J. Appl. Crystallogr. 8* (1975) 568.
10. Johnson, C. K. *ORTEP: A Fortran Ellipsoid Plot Program for Crystal Structure Illustrations,* Report ORNL-3794, Second Rev., Oak Ridge National Laboratory, Oak Ridge 1970.
11. Stewart, J.M. *et al. The X-Ray System 1972,* Technical Report TR-192, Computer Science Center, University of Maryland, College Park 1972.
12. Germain, G., Main, P. and Woolfson, M.M. *Acta Crystallogr. A 27* (1971) 368.
13. Cromer, D.T. and Mann, J. B. *Acta Crystallogr. A 24* (1968) 321.
14. Cromer, D. T. and Liberman, D. *J. Chem. Phys. 53* (1970) 1891.
15. Michelsen, K. and Pedersen, E. *Acta Chem. Scand. A 32* (1978) 847.
16. Rotenberg, M., Bivins, R., Metropolis, N. and Wooten, J. K., Jr. *The 3-j and 6-j Symbols,* MIT Press, Cambridge 1959.
17. Wigner, E. P. *Group Theory and its Application to the Quantum Mechanics of Atomic Spectra,* Academic, New York 1959.
18. Silver, B. L. *Irreducible Tensor Methods, An Introduction for Chemists,* Academic, New York 1976.
19. Fano, U. and Racah, G. *Irreducible Tensorial Sets,* Academic, New York 1959.
20. Thaddeus, P., Krisher, L. C. and Loubser, J. H. N. *J. Chem. Phys 40* (1964) 257.
21. Damhus, T. *Thesis,* University of Copenhagen, Copenhagen 1984.
22. Güdel, H. U., Hauser, U. and Furrer, A. *Inorg. Chem. 18* (1979) 2730.
23. Güdel, H. U. and Hauser, U. *Inorg. Chem. 19* (1980) 1325.
24. Güdel, H. U. and Hauser, U. *Theor. Chim. Acta 62* (1983) 319.
25. Güdel, H. U. and Hauser, U. *J. Solid State Chem. 35* (1980) 230.
26. Jotham, R.W. and Kettle, S. F. A. *Inorg. Chim. Acta 4* (1970) 145.
27. Sinn, E. *Coord. Chem. Rev. 5* (1970) 313.
28. O'Connor, C. J. *Progr. Inorg. Chem. 29* (1982) 203.
29. Hatfield, W. E. In Boudreaux, E. A. and Mulay, L. N., Eds., *Theory and Applications of Molecular Paramagnetism,* Wiley, London 1976, Chapter 7.
30. Hauser, U. *Diss.,* Universität Bern, Bern 1979.
31. Griffith, J. S. *Struct. Bond. 10* (1972) 87.
32. Wieghardt, K., Schmidt, W., Endres, H. and Wolfe, C. R. *Chem. Ber. 112* (1979) 2837.
33. Hodgson, D. J. and Pedersen, E. *Inorg. Chem. 19* (1980) 3116 and references therein.
34. Cline, S. C., Hodgson, D. J., Kallesøe, S., Larsen, S. and Pedersen, E. *Inorg. Chem. 22* (1983) 637.
35. Werner, A. *Ber. Dtsch. Chem. Ges. 40* (1907) 2103.
36. Jørgensen, S. M. *Z. Anorg. Allg. Chem. 16* (1898) 184.
37. Jørgensen, S. M. *J. Prakt. Chem. 45* (1892) 260.
38. Mønsted, L. and Mønsted, O. *Acta Chem. Scand. A 32* (1978) 917.
39. Bang, E. *Acta Chem. Scand. 22* (1968) 2671.
40. Bang, E. and Narasimhayya, T. *Acta Chem. Scand. 24* (1970) 275.
41. Bang, E. *Acta Chem. Scand. A 38* (1984) 417
42. Pfeiffer, P., Vorster, W. and Stern, R. *Z. Anorg. Allg. Chem. 58* (1908) 272.

43. Flood, M. T., Marsh, R. E. and Gray, H. B. *J. Am. Chem. Soc. 91* (1969) 193.
44. Güdel, H. U., Furrer, A. and Murani, A. *J. Magn. Magn. Mater. 15–18* (1980) 383.
45. Furrer, A., Güdel, H. U. and Hauser, U. *J. Appl. Phys. 50* (1979) 2043.
46. De Wolff, P. M. *J. Appl. Crystallogr. 1* (1968) 108.

Received August 5, 1983.